Temperature effect on the submicron AlGaN/GaN Gunn diodes for terahertz frequency

Lin'an Yang,[a] Wei Mao, Qingyang Yao, Qi Liu, Xuhu Zhang, Jincheng Zhang, and Yue Hao

State Key Discipline Laboratory of Wide Band Gap Semiconductor Technology, Xidian University, Xi'an 710071, China

(Received 24 February 2010; accepted 6 December 2010; published online 19 January 2011)

The wurtzite AlGaN/GaN Gunn diode with tristep-graded Al composition AlGaN as hot electron injector is simulated by using an improved negative differential mobility model of GaN. The results show that the oscillation mode of Gunn diode gradually shifts from dipole domain mode toward accumulation mode with increase in temperature, and the mode shift closely depends on the injector length. At the temperatures of 300–400 K, 0.6 and 0.4 μm Gunn diodes normally generate the oscillation of dipole domain mode, yielding the fundamental oscillation frequencies of 332–352 GHz and 488–508 GHz, respectively, with the dc/rf conversion efficiencies of 2%–3% and the output power densities of 10^9–10^{10} W cm^{-3}. At higher temperatures, the diodes generate the accumulation mode oscillation, and the highest frequency approaches 680 GHz and 977 GHz, respectively, with the dc/rf conversion efficiencies of 0.5%–1%. © *2011 American Institute of Physics*. [doi:10.1063/1.3533984]

I. INTRODUCTION

Gallium nitride (GaN) based Gunn diode has shown the potential of generating high oscillation frequency and high output power therefore it is one of the promising candidates for application in solid-state source of terahertz radiation. Previous simulations demonstrated that the bulk GaN Gunn diode with around 1 μm long transit region including doping notch or doping spike can generate the oscillation frequencies of 200–250 GHz.[1–4] From a simple estimation by $f=v_{sat}/L$, where the saturation drift velocity $v_{sat}\approx 2\times 10^7$ cm/s for wurtzite GaN, the transit region length (L) of less than 0.7 μm is necessary to lift the frequency up to 300 GHz. However, it is difficult to sustain the Gunn oscillation in conventional $n^+/n/n^+$ structure Gunn diode with such a short transit region because the injected electrons cannot obtain enough energy to create the intervalley transfer from central Γ-valley into upper valley so as to form the high field domain. Thus an additional electron launching layer, i.e., hot electron injector, is required to configure $n^+/n^-/n/n^+$ structure in order to form a stable Gunn oscillation. The work of Förster *et al.*[5] demonstrated the outstanding performance of GaAs Gunn diode with AlGaAs as hot electron injector. The AlGaAs barrier can supply lots of "hot" electrons into the transit region to promote the intervalley electron transfer therefore reduce the length of "dead zone" from the beginning of the transit region. As a result, the Gunn diode can present the outstanding noise performance, temperature stability, and power conversion efficiency. So far use of AlGaN as hot electron injector to promote the formation of dipole domain in GaN Gunn diode is seldom discussed. Indeed, there also exists a limited space-charge accumulation (LSA) mode oscillation for submicron GaN diode without hot electron injector, under the condition of $N\times L<5.2\times 10^{12}$ cm^{-2}, where N and L are the doping concentration and the transit region length, respectively.[6–8] In this work, we employ an improved negative differential mobility model to simulate the performance of submicron GaN Gunn diode operating at terahertz frequencies. A barrier layer of AlGaN with tristep-graded Al composition is proposed as the hot electron injector, aimed at promoting the dipole domain mode oscillation by means of the large band gap offset of AlGaN/GaN heterostructure. A wide range of temperature (300–450 K) is included in simulation since the Gunn diode never operates at room temperature due to low dc/rf conversion efficiency.

II. MODEL DESCRIPTION

A. Negative differential mobility model

The dependence of carrier drift velocity on electric field for bulk GaN material was investigated by lots of Monte Carlo (MC) simulations. Based on these results, a semianalytical model of negative differential mobility, as is called Farahmand Modified Caughey Thomas (FMCT) mobility model hereafter, was developed which includes low field and high field mobility models [see Eqs. (2) and (3) in Ref. 9]. In this work, we first improve the parameters of FMCT mobility model especially the high field mobility model according to the recent MC simulation data that took more reasonable band structure and scattering mechanisms into account, then employ the model to simulate the performance of GaN Gunn diode. In FMCT high field mobility model, the parameters such as the critical electric field E_{crit}, the saturation drift velocity v_{sat} and other curve fitting parameters were defined as constants, which have been found to cause significant error at high temperatures.[10] Thus we introduce the temperature dependent parameters in the model to overcome the weakness of FMCT mobility model. We use the improved model to fit the MC simulation data,[11] and obtain the temperature

[a]Electronic mail: layang@xidian.edu.cn.

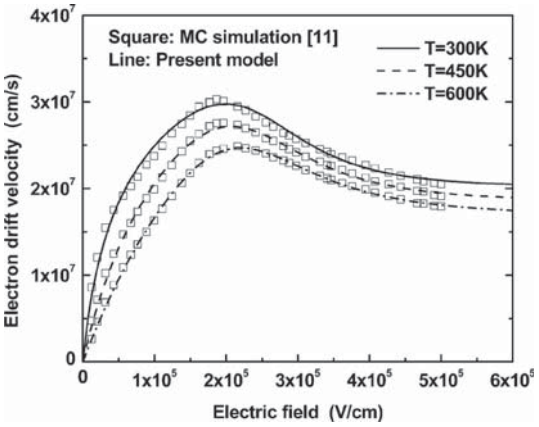

FIG. 1. Temperature dependence of high-field transport characteristics of bulk wurtzite n-GaN doped at $\sim 10^{17}$ cm^{-3} calculated by present model and MC data.

dependent parameters as follows: the dimensional parameters $E_{\text{crit}}=1.985\times10^5\times T_E(\text{V/cm})$, $v_{\text{sat}}=2.016\times10^7\times T_v(\text{cm/s})$, and the dimensionless parameters $n_1=6.052\times T_{n1}$, $n_2=0.856\times T_{n2}$, $a=4.592\times T_a$, where the dimensionless coefficients T_E, T_v, T_{n1}, T_{n2}, and T_a are given as follows with T given in Kelvin:

$$T_E = 0.745 + 9.501\times10^{-4}\ T - 3.221\times10^{-7}\ T^2, \quad (1)$$

$$T_v = 1.048 - 9.988\times10^{-6}\ T - 4.994\times10^{-7}\ T^2, \quad (2)$$

$$T_{n1} = 0.946 - 5.055\times10^{-4}\ T - 1.082\times10^{-6}\ T^2, \quad (3)$$

$$T_{n2} = 0.934 - 1.332\times10^{-4}\ T + 1.211\times10^{-6}\ T^2, \quad (4)$$

$$T_a = 5.533 - 2.613\times10^{-2}\ T + 4.471\times10^{-5}\ T^2, \quad (5)$$

where T_E indicates a nearly linear increase in critical electric field with temperature which was explained theoretically in Ref. 11. T_v presents a nearly linear decrease in electron saturation drift velocity with rising temperature. It is due to that the electric field corresponding to the saturation drift velocity is far beyond the negative differential resistance (NDR) region, in which case the intervalley scattering exceeds the polar-optical phonon scattering therefore becomes the dominant scattering mechanism. The enhancement of the intervalley scattering with temperature promotes the random scattering in turn reduces the drift velocity along the electric field direction.[12] T_{n1} demonstrates a negative temperature dependence of n_1 which means higher saturation electric field E_{sat} is required to sustain the stationary state of nonequilibrium carrier system as the temperature rises. T_{n2} and T_a show more mathematical than physical meaning and are used to modify the velocity-field curve near the critical electric field. With these improved parameters, we simulate the velocity versus field dependence of wurtzite GaN at different temperatures. The result is given in Fig. 1, showing a good agreement between our simulation and MC data.

Comparing to recent MC simulations,[9,10,13–16] the MC simulation in Ref. 11 slightly overestimates the electron drift velocity at room temperature. The difference attributes to using different carrier scattering and band structure of GaN in simulations. Thus, we extract more accurate parameters from recent MC simulations as follows: $E_{\text{crit(GaN)}}=2.209\times10^5\times T_E(\text{V/cm})$, $v_{\text{sat(GaN)}}=1.907\times10^7\times T_v(\text{cm/s})$, $n_{1(\text{GaN})}=7.143\times T_{n1}$, $n_{2(\text{GaN})}=0.783\times T_{n2}$, and $a_{(\text{GaN})}=5.362\times T_a$. The temperature coefficients T_E, T_v, T_{n1}, T_{n2}, and T_a are still determined by Eqs. (1)–(5) because the simulation of temperature effect in Ref. 11 is regarded as reasonable. According to the MC data concerning the AlGaN with 20%, 50%, and 80% Al compositions,[9] we use the interpolation calculation to determine the AlGaN mobility model. The Al composition dependent parameters for wurtzite AlGaN doped at $\sim10^{17}$ cm^{-3} are given as

$$E_{\text{crit(AlGaN)}} = (1 + 0.818x + 0.341x^2)\times E_{\text{crit(GaN)}}, \quad (6)$$

$$\nu_{\text{sat(AlGaN)}} = (1 + 0.365x - 0.226x^2)\times \nu_{\text{sat(GaN)}}, \quad (7)$$

$$n_{1(\text{AlGaN})} = (1 + 1.325x - 3.154x^2)\times n_{1(\text{GaN})}, \quad (8)$$

$$n_{2(\text{AlGaN})} = (1 + 0.575x - 0.311x^2)\times n_{2(\text{GaN})}, \quad (9)$$

$$a_{(\text{AlGaN})} = (1 - 0.417x + 0.424x^2)\times a_{(\text{GaN})}, \quad (10)$$

where x is the Al composition. For low field mobility μ_0, different from the previous work,[17] we have developed a parabolic modifying factor of electron effective quality m^* to characterize the variation in μ_0 with doping concentration and temperature. The results agree well with that in FMCT mobility model.

B. Interface charge model of AlGaN/GaN heterostructure

In this work, a barrier layer of $Al_xGa_{1-x}N$ with tristep-graded Al composition ($x=1\%$, 8%, and 15%) is proposed as the hot electron injector of GaN Gunn diode. The influence of polarization induced interface charge in the AlGaN/GaN heterostructure should be taken into account, which will be discussed in Sec. III. In simulation, the interface charge in the AlGaN layer is regarded as the positive sheet charge near AlGaN/GaN interface. The sheet charge density σ varies with Al composition x so that is modeled by[18]

$$\sigma(x) = P_{\text{SP}}(\text{GaN}) - P_{\text{SP}}(Al_xGa_{1-x}N) - P_{\text{PE}}(Al_xGa_{1-x}N), \quad (11)$$

where $P_{\text{SP}}(\text{GaN}) - P_{\text{SP}}(Al_xGa_{1-x}N) = 0.052x$ is the interface charge induced by spontaneous polarization, $P_{\text{PE}}(Al_xGa_{1-x}N)$ is the piezoelectric polarization induced charge modeled by

$$P_{\text{PE}}(Al_xGa_{1-x}N) = 2\frac{a(0)-a(x)}{a(x)}\left[e_{31}(x) - e_{33}(x)\frac{C_{13}(x)}{C_{33}(x)}\right], \quad (12)$$

where $a(0)$ and $a(x)$ are the crystal lattice constants, $C_{13}(x)$ and $C_{33}(x)$ are the elastic constants, $e_{31}(x)$ and $e_{33}(x)$ are the piezoelectric coefficients, respectively. A linear interpolation has been employed to calculate these parameters for AlGaN.[19]

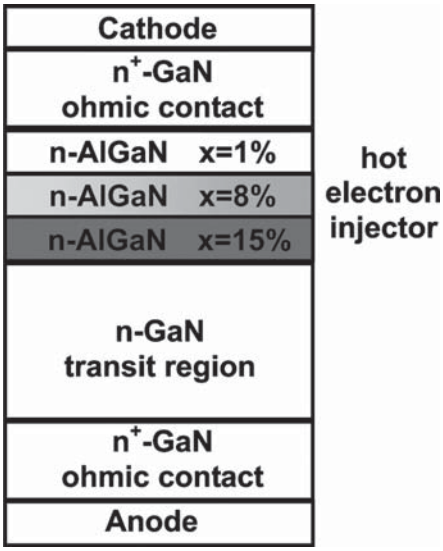

FIG. 2. Section structure of GaN Gunn diode with a tristep-graded Al composition n-AlGaN as hot electron injector.

C. Simulation method

Above analytical models are embedded into SILVACO simulator in order to increase the calculation efficiency. We use a "self-excitation oscillation" method to evaluate the maximal output capability of Gunn diode which can be realized by supplying an appropriate dc bias voltage across the terminals of the diode, instead of connecting the Gunn diode with a RLC resonant circuit that was widely used in previous MC simulations. The dc bias voltage is adjusted to assure the internal electric field located at the NDR region. In this case, the NDR compensates the positive resistance consisting of bulk resistance and contact resistance, and then forms the oscillation. By steady-state and instantaneous simulations, the dc and ac voltages and currents at the terminals of diode are obtained. The dc dissipated power P_{dc}, rf peak power $P_{rf(peak)}$, and corresponding fundamental frequency f_{osc} can be extracted by using a fast Fourier transform algorithm, accordingly the dc/rf conversion efficiency can be approximately calculated by using $\eta = P_{rf}/P_{dc} = [P_{rf(peak)}/8]/(V_{dc} \times I_{av})$. Although the oscillation frequency cannot be tuned within a wide range, the self-excitation oscillation method reveals the maximal oscillation capability of Gunn diode meanwhile the simulation procedure shows higher calculation efficiency, which is suitable for the device-fabrication-oriented simulation.

III. RESULTS AND DISCUSSION

A. Effect of polarization charge

The section structure of AlGaN/GaN Gunn diode in our simulation is shown in Fig. 2. The n-AlGaN hot electron injector locates between the cathode Ohmic contact layer and the transit region layer. It includes the trigraded Al composition of 1%, 8%, and 15% respectively, where the 1% Al layer acts more as a spacer layer to prevent the dopant diffusion from n^+-GaN to n-AlGaN, the 8% Al layer is a doping transition layer, and the 15% Al layer eventually forms a heterostructure with GaN active layer. As a result, the electron accumulation appears in the GaN region adjacent to the heterointerface because of strong piezoelectric and spontaneous polarizations. Different from that in AlGaN/GaN high electron mobility transistor (HEMT), it does not create a high density two-dimensional electron gas since the GaN transit region is a conductive layer in Gunn diode while the GaN buffer is a semi-insulating layer in HEMT. Under the drive of built-in electric field induced by the AlGaN/GaN band gap offset as well as the external electric field supplied by the bias voltage, lots of electrons earn enough energy to form the Gunn domain. Actually, the heterostructure induced electron accumulation has the similar role as n^+-spike doping layer that is used to suppress the "depletion zone" in AlGaAs/GaAs Gunn diode.[5,20] To estimate the effect of polarization in GaN Gunn diode, we consider different conditions in simulation, i.e., one with polarization effect, one without polarization effect as well as one using n^+-spike doping layer instead of polarization effect. The diode is composed of 0.5 μm long cathode n^+-GaN Ohmic contact layer doped at 2.5×10^{18} cm^{-3} with a specific contact resistivity of 5×10^{-6} Ω cm^2 to electrode, 50 nm long tristep-graded n-AlGaN injector (10 nm 1% Al layer, 20 nm 8% Al layer, and 20 nm 15% Al layer) doped at 5×10^{16} cm^{-3} followed by 0.6 μm long n-GaN transit region doped at 1.5×10^{17} cm^{-3}, and 0.5 μm long anode n^+-GaN Ohmic contact layer. For the diode with n^+-spike doping layer, an additional 10 nm long n^+-GaN layer doped at 2×10^{18} cm^{-3} is inserted between injector layer and transit layer. Figure 3 gives the simulated electron concentration and electric field distributions near the heterointerface at room temperature. It is found that the diode with polarization effect and the diode with n^+-GaN spike doping layer demonstrate the similar electron concentration and electric field distributions in the AlGaN layers while the diode without polarization effect presents an evident difference. Further instantaneous simulation proves that the diode with polarization and the diode with spike doping easily generate the stable oscillation at dipole domain mode while the diode without polarization usually fails in Gunn oscillation. It indicates that the polarization effect can suppress the formation of depletion in the transit region thereby compensate the lack of high energy electrons. The induced electrons indeed act as same as those in n^+-spike layer. So the AlGaN/GaN Gunn diode with even a very short transit region can promote the formation and the propagation of dipole domain, although no n^+-spike layer is employed.

B. Effect of temperature on the oscillation mode

The AlGaN/GaN Gunn diodes with 0.4 and 0.6 μm long transit regions are investigated in this work. The shorter transit region is not discussed because our work put the emphasis on the Gunn mode instead of LSA mode oscillation. A dc bias voltage across the diode is adjusted to generate the self-excitation oscillation. After that an instantaneous simulation sustains the time period of 100 ps to obtain the ac voltage and current oscillation waveforms. Meanwhile, the electron concentration and electric field distributions are extracted to

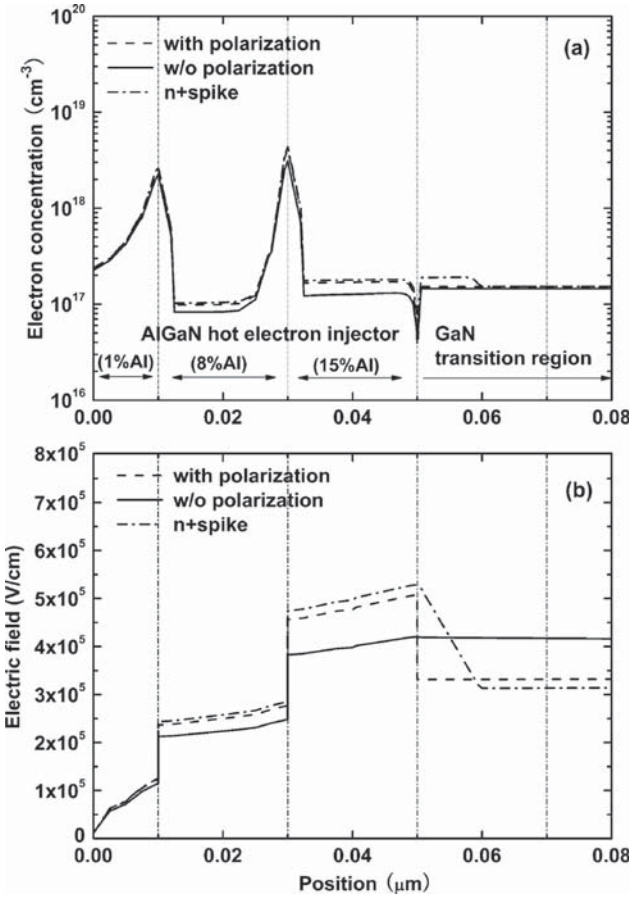

FIG. 3. Room temperature electron concentration and electric field distributions of AlGaN/GaN Gunn diode extracted from instantaneous simulation under the dc bias voltage of 26 V.

estimate the oscillation mode. Because of low dc/rf conversion efficiency of the real Gunn diode, the investigation of the GaN Gunn diode operating at the temperatures of 300–450 K is the emphasis of this work.

At first, the AlGaN/GaN Gunn diode with 0.6 μm long and 1.5×10^{17} cm^{-3} doped transit region is simulated at the temperatures ranging from 300 to 450 K, where the injector doping is set as 5×10^{16} cm^{-3} and the injector length varies from 30 to 200 nm. The dependence of dc I-V characteristic of the Gunn diode on temperature is shown in Fig. 4, where the knee point indicates the threshold of generating NDR oscillation. It is found that higher dc bias and higher dc current are required to form the stable NDR oscillation with increase of temperature, which attributes to the degradation of NDR performance at high temperature (see Fig. 1). Therefore, the dc dissipated power significantly increases as such the dc/rf conversion efficiency decreases. In instantaneous simulation, the dc bias voltage across the diode is set as 26 V to assure the bias located at the NDR region of velocity-field curve so as to generate a stable oscillation. It is found that the oscillation mode varies with both AlGaN injector length and temperature. As validation, the different electric field distributions are extracted by the time step of 250 fs from instantaneous simulation with the results shown in Fig. 5, representing the dipole domain mode, the dipole-accumulation transition mode as well as the accumulation

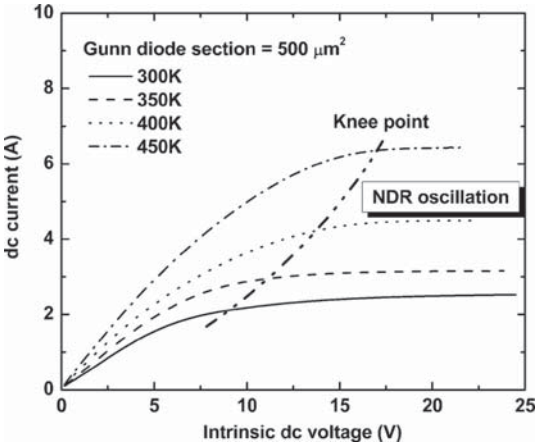

FIG. 4. Variation of dc I-V characteristic with temperature for 0.6 μm AlGaN/GaN Gunn diode with AlGaN injector length of 200 nm. The diode section area is set to be 500 μm^2.

mode, respectively. The corresponding oscillation frequency increases with the oscillation mode changing from dipole domain to accumulation, which is understandable because the electron depletion does not appear in accumulation mode so the electron transit period is shorter. The output performances of the diodes with different injector lengths are simulated with the results given in Fig. 6, where (a) shows the temperature dependence of the fundamental oscillation frequency, meanwhile the corresponding oscillation modes are marked, (b) gives the corresponding output power density and dc/rf conversion efficiency. It is found that the oscillation mode gradually shifts from dipole domain mode toward accumulation mode and the trend of mode shift depends on the injector length as the temperature rises. At dipole domain mode, the fundamental oscillation frequencies of 332–352 GHz are consistent with the approximate estimation by f_{osc}

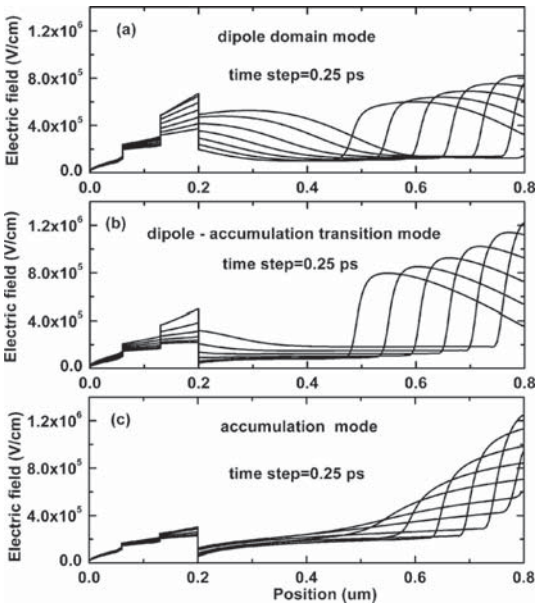

FIG. 5. Electric field distribution in AlGaN injector and GaN transit region extracted from instantaneous simulation (time step=250 fs for curve spacing) to indicate the oscillation at (a) dipole domain mode, (b) dipole-accumulation transition mode, and (c) accumulation mode, respectively.

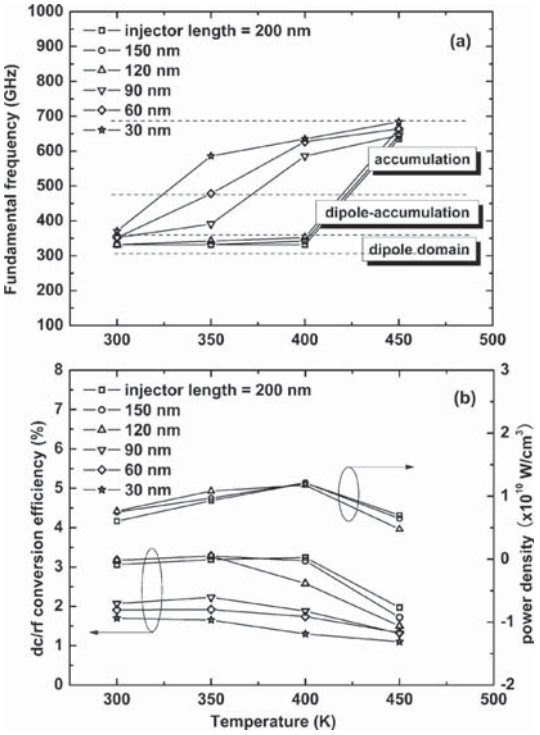

FIG. 6. Temperature dependence of (a) fundamental frequency, (b) rf power density, and dc/rf conversion efficiency for 0.6 μm AlGaN/GaN Gunn diode, where the AlGaN injector length ranges from 30 to 200 nm.

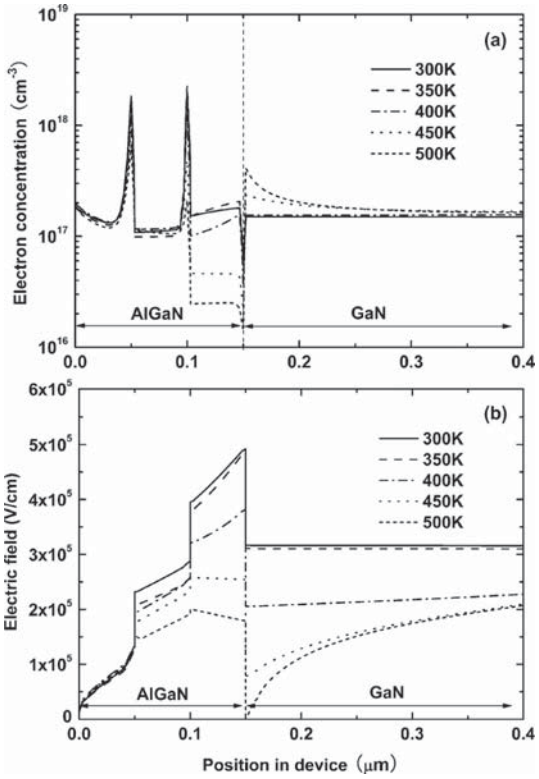

FIG. 7. Temperature dependence of (a) electron concentration distribution, (b) electric field distribution at the AlGaN/GaN interface for 0.6 μm AlGaN/GaN Gunn diode with injector length of 150 nm.

$=v_{sat}/L$. The dipole-accumulation transition mode presents a significant increase of frequency. At accumulation mode, the oscillation frequency is higher than 500 GHz and the maximal frequency approaches to 700 GHz. The power performance gives that the GaN Gunn diode working at dipole domain mode presents higher conversion efficiency ($\sim$3%) than that of accumulation mode ($\sim$1%), and the rf power density of 10^9–10^{10} W/cm^3 is two orders of magnitude larger than that of GaAs Gunn diode. Note that the outstanding output performance of GaN Gunn diode is obtained under the optimal oscillation condition because we employ the self-excitation oscillation method in simulation. In fact, the assembly of external RLC resonance circuit in the real oscillator could degrade the output performance. One reason is that the external components introduce additional power dissipation. The other is that the circuit tuning throughout the frequency band can hardly deliver the maximal output capability of the device. It is also found that the shift of oscillation mode is sensitive to the injector length. Figure 6(a) shows that the Gunn diode with injector length of 120–200 nm can generate a stable dipole domain mode oscillation within the temperature range of 300–400 K, the practical temperature range of Gunn diode. When the injector length shrinks below 90 nm, the oscillation mode demonstrates a significant shift even in the normal temperature range. Specially, the oscillation monotonously occurs at accumulation mode with frequency up to 680 GHz and dc/rf conversion efficiencies of 1.1%–1.3% when the injector length shrinks to 30 nm. Clearly the accumulation mode of this kind is capable of generating extremely high frequency signal and it is easily realized compared with the LSA mode. Therefore, it can be used to generate high fundamental frequency with high output power instead of frequency multiplier. To deeply explain the shift of oscillation mode with temperature, Fig. 7 gives the simulated electron concentration and electric field in AlGaN injector and GaN transit region at different temperatures (300–500 K). As the temperature rises, it trends to evident accumulation of electron and nonuniformity of electric field in the transit region adjacent to the AlGaN/GaN interface. When the temperature is below 400 K, it can yet form the uniform electric field distribution in the transit region so that the dipole domain oscillation can be sustained. With the temperature increasing to some extent (>400 K), the electric field near the interface shows a significant decrease thereby causes the nonuniform distribution and electron accumulation. It weakens the energy of electrons at the beginning of the transit region accordingly impacts on the formation and propagation of dipole domain. This kind of phenomenon usually appears when the transit region is very short. It is basically due to the degradation of NDR characteristics at high temperature. In this case, the injector length is a key parameter to modulate the electric field distribution and determine the energy of accelerated electrons in the transit region of Gunn diode.

Second, the AlGaN/GaN Gunn diode with 0.4 μm long and 1.5×10^{17} cm^{-3} doped transit region is simulated with the frequency and power performances given in Fig. 8. According to the dc I-V characteristic, the dc bias voltage across the diode is set as around 21 V to sustain a stable oscillation. It is found that the diode can generate the dipole

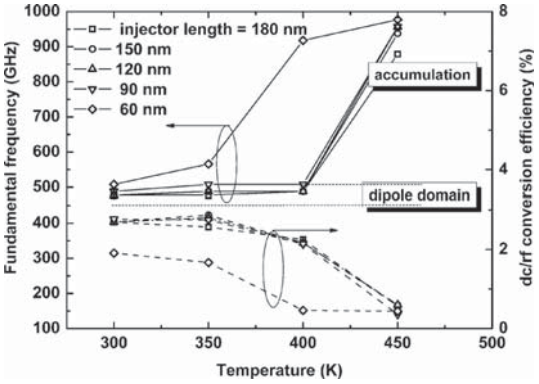

FIG. 8. Temperature dependence of fundamental frequency and dc/rf conversion efficiency for 0.4 μm AlGaN/GaN Gunn diode, where the AlGaN injector length ranges from 60 to 180 nm.

domain oscillation at 488–508 GHz when the AlGaN injector length varies from 90 to 180 nm at 300–400 K. The maximal dc/rf conversion efficiency is lower than that of 0.6 μm diode yet is larger than 2%. On the other hand, the maximal fundamental frequency approaches 977 GHz accompanying with the efficiency of around 0.5% at the accumulation mode, which is approaching to the result in Ref. 8. When the injector length is less than 60 nm, it is hard to generate the self-excitation oscillation at any mode in our simulation because it is difficult to modulate the electric field distribution to form the domain in such a short transit region. Obviously the GaN Gunn diode with shorter transit region trends to work at the LSA mode[6–8] under the external ac stimulation.

IV. SUMMARY

The submicron GaN Gunn diode with a tristep-graded Al composition (1%, 8%, and 15%) AlGaN buffer layer as hot electron injector has been simulated by using an improved negative differential mobility model. The model takes the AlGaN/GaN heterostructure induced polarization effect and the temperature effect into account. A self-excitation oscillation method with higher calculation efficiency is used in simulation to form a stable oscillation so as to obtain the optimal oscillation capability of GaN Gunn diode. The simulation results show that the high frequency oscillation gradually shifts from dipole domain mode toward accumulation mode with increase in temperature, and the trend of mode shift closely depends on the AlGaN injector length. For 0.6 μm GaN Gunn diode, it is found that the 120–200 nm long AlGaN injectors can sustain the dipole domain oscillation at 332–352 GHz within the temperature range of 300–400 K. The rf power density of 10^9–10^{10} W/cm^3 and the dc/rf conversion efficiency of around 3% are obtained at the optimal oscillation. The shorter AlGaN injector (<60 nm) can easily generate the accumulation mode oscillation with fundamental frequency up to 680 GHz and the conversion efficiency of around 1%. For 0.4 μm Gunn diode, it is yet possible to generate the stable dipole domain mode oscillation at 300–400 K with the fundamental frequencies of 488–508 GHz, and the maximal conversion efficiency is larger than 2%. The accumulation mode oscillation yields the frequency approaching to 977 GHz with the conversion efficiency of around 0.5%. Although the dipole domain mode oscillation with outstanding output performance is normally concerned for Gunn diode, the accumulation mode oscillation easily delivers higher fundamental frequency so it can be used in terahertz domain instead of conventional frequency multiplier.

ACKNOWLEDGMENTS

This work was supported by the National Natural Science Fund of China (Grant No. 61076079), the Key Program of National Natural Science Fund of China (Grant No. 60736033), and the National Key Science & Technology Special (Grant No. 2008ZX01002-002).

[1]V. Gruzinskis, P. Shiktorov, E. Starikov, and J. H. Zhao, Semicond. Sci. Technol. **16**, 798 (2001).
[2]R. F. Macpherson, G. M. Dunn, and N. J. Pilgrim, Semicond. Sci. Technol. **23**, 055005 (2008).
[3]R. F. Macpherson and G. M. Dunn, Appl. Phys. Lett. **93**, 062103 (2008).
[4]L. A. Yang, Y. Hao, and J. C. Zhang, Appl. Phys. Lett. **95**, 143507 (2009).
[5]A. Förster, M. I. Lepsa, D. Freundt, J. Stock, and S. Montanari, Appl. Phys. A: Mater. Sci. Process. **87**, 545 (2007).
[6]V. N. Sokolov, K. W. Kim, V. A. Kochelap, and D. L. Woolard, J. Appl. Phys. **98**, 064507 (2005).
[7]E. A. Barry, V. N. Sokolov, K. W. Kim, and R. J. Trew, J. Appl. Phys. **103**, 126101 (2008).
[8]E. A. Barry, V. N. Sokolov, K. W. Kim, and R. J. Trew, Appl. Phys. Lett. **94**, 222106 (2009).
[9]M. Farahmand, C. Garetto, E. Bellotti, K. F. Brennan, M. Goano, E. Ghillino, G. Ghione, J. D. Albrecht, and P. P. Ruden, IEEE Trans. Electron Devices **48**, 535 (2001).
[10]F. Schwierz, Solid-State Electron. **49**, 889 (2005).
[11]J. D. Albrecht, R. P. Wang, P. P. Ruden, M. Farahmand, and K. F. Brennan, J. Appl. Phys. **83**, 4777 (1998).
[12]S. Chen and G. Wang, J. Appl. Phys. **103**, 023703 (2008).
[13]A. Reklaitis and L. Reggiani, J. Appl. Phys. **95**, 7925 (2004).
[14]Y. Tomita, H. Ikegami, and H. I. Fujishiro, Phys. Status Solidi C **4**, 2695 (2007).
[15]F. Bertazzi, M. Moresco, and E. Bellotti, J. Appl. Phys. **106**, 063718 (2009).
[16]F. Djeffal, N. Lakhdar, M. Meguellati, and A. Benhaya, Solid-State Electron. **53**, 988 (2009).
[17]H. Arabshahi, Turk. J. Phys. **33**, 219 (2009).
[18]O. Ambacher, B. Foutz, J. Smart, J. R. Shealy, N. G. Weimann, K. Chu, M. Murphy, A. J. Sierakowski, W. J. Schaff, L. F. Eastman, R. Dimitrov, A. Mitchell, and M. Stutzmann, J. Appl. Phys. **87**, 334 (2000).
[19]A. E. Romanov, T. J. Baker, S. Nakamura, and J. S. Speck, J. Appl. Phys. **100**, 023522 (2006).
[20]S. Montanari, A. Förster, M. I. Lepsa, and H. Lüth, Solid-State Electron. **49**, 245 (2005).